

RAS 11919

DOCKETED
USNRC

UNITED STATES OF AMERICA

June 30, 2006 (4:43pm)

NUCLEAR REGULATORY COMMISSION

OFFICE OF SECRETARY
RULEMAKINGS AND
ADJUDICATIONS STAFF

_____)	
In the Matter of)	Docket No. 40-8838-MLA
)	
U.S.ARMY)	ASLBP No. 00-776-04-MLA
)	
(Jefferson Proving Ground Site))	June 30, 2006

**MOTION FOR LEAVE TO FURTHER SUPPLEMENT
CONTENTIONS OF SAVE THE VALLEY, INC. WITHIN SIXTY (60) DAYS**

Pursuant to 10 C.F.R. § 323, Petitioner Save the Valley, Inc. ("STV") respectfully moves for leave to further supplement within sixty (60) days, pursuant to 10 C.F.R. § 2.309(f), its contentions and/or bases for hearing, as initially filed in this matter on November 23, 2005 ("Initial Contentions") and subsequently modified on May 31 2006 ("Final Contentions"), to address the significant implications of three new sources of information which only recently became available to STV.

In support of its Motion, STV would respectfully show the Board:

1. On May 19, 2006, Scientific Applications International Corporation ("SAIC") forwarded to the NRC Staff on behalf of the Army its *Final Report, Environmental Radiation Monitoring Report for License SUB-1435, Jefferson Proving Ground, Summary of Results for October 17-20, 2005 Sampling Event* ("October 2005 Monitoring Report"). Even though this report was expressly submitted "[i]n accordance with the U.S. Army's direction and in support of its request for termination of the Jefferson Proving Ground (JPG) License SUB-1435 under restricted release conditions," the document was not served on or otherwise provided to STV by SAIC or the Army. As a result, it was not until STV made a routine search of ADAMS on June 5, 2006, for new postings relating to the JPG site that STV discovered a copy of the report (Accession No.

TEMPLATE = SELV-037

SELV-02

ML061430302) and was able to distribute the document to its experts for expedited review.¹

2. On June 13, 2006, SAIC forwarded to the NRC Staff on behalf of the Army its the Fracture Trace Analysis (SAIC, June, 2006). Even though this report was expressly submitted as an addendum to the Field Sampling Plan (“FSP”) at issue in this proceeding, the document was not served on or otherwise provided to STV by SAIC or the Army. It was not posted to ADAMS until June 16, 2006. As a result, it was not until STV made a routine search of ADAMS on June 18, 2006, for new postings relating to the JPG site that STV discovered a copy of the report (Accession No. ML061670091) and was able to distribute the document to its experts for expedited review.²

3. On June 4, 2006, STV received notice for the first time of a research paper recently published by V. H. Coryell and D. M. Stearns, “Molecular analysis of hprt mutations generated in Chinese Hamster Ovary EM9 cells by uranyl acetate, by hydrogen peroxide and spontaneously” (Molec. Carcinogen. 2006. 45:60-72) (copy attached). As a result, it was not until June 5, 2006, that STV was able to distribute the document to its experts for expedited review.

4. Each of these sources, when evaluated in context with other existing information

¹In this regard, it should be noted that the October 2005 Monitoring Report expressly states that the sampling whose results are being reported was conducted in accordance with the protocols specified in the Army’s 2003 Environmental Radiation Monitoring Program, as modified in April, 2004. However, within a week of SAIC’s submission of the Report, the Army submitted an errata letter to the NRC Staff stating that this statement was in error, and that the correct protocols were identified in a two page attachment – but the attachment was missing. See ML061640195, submitted May 26, 2006, but not posted to ADAMS until June 13, 2006. Upon inquiry to the NRC Staff, STV was advised that the missing two-page attachment would not be available on ADAMS until the week of July 3, 2006.

²It should be noted that there are reviewer notes for the Fracture Trace Analysis which have not been posted to ADAMS along with the Analysis. These reviewer notes are especially significant to STV’s further review of the Analysis and assessment of its implications. However, STV has, to date, been unable to determine from inquiry to the NRC Staff when, or even if, these notes will be posted to ADAMS.

available from JPG and/or earlier scientific literature, materially impacts the understanding of the JPG facility with respect to the issues related to depleted uranium (DU) on the site, the migration of uranium from the site, the ability of the field sampling plan, as it is being implemented, to accomplish its objectives with respect to the migrating uranium, and the biological risks associated with the migrating uranium. *See* attached Verified Statement of Charles H. Norris, ¶ 5.

5. In short, the October 2005 Monitoring Report results (if reliable) appear to show that depleted uranium has migrated to the JPG site boundaries in at least two media and that a previously unidentified source or sources of enriched uranium is present at the JPG site. The fracture trace analysis report, central to the FSP approach to characterization of the JPG site, shows that the analysis was not performed as proposed in the FSP, and cannot perform the critical purpose it was intended to serve. The recent Coryell and Stearns research demonstrates a previously unidentified and unevaluated risk to human health and the environment from the DU at JPG. Together, these three new sources of information, when evaluated in context with other existing information available from JPG and/or earlier scientific literature, materially impact the understanding of the JPG facility with respect to the risks to human health and the environment related to depleted (and other) uranium on the JPG site, the migration of uranium from the site, and the biological risks associated with the migrating uranium. They also impact the ability of the FSP, as it is designed and being implemented, to accomplish its objectives with respect to the migrating uranium and the biological risks associated with the migrating uranium. *See* Norris Verified Statement, ¶ 21

6. Given the short period of time since STV received these three new sources of information, it has simply not been feasible for STV and its experts to assess all of their implications for the characterization of the JPG site and then formulate those implications in

contentions and bases meeting the format and content requirements of the NRC rules by June 30, 2006. But, there is no doubt that these implications are quite significant. In the first place, the reported presence of DU at the JPG site boundaries raises significant issues regarding the need for environmental radiation monitoring and field sampling outside the JPG site boundaries. In the second place, assuming the reliability of the SAIC results, the evidence of enriched uranium within the JPG site boundaries poses significant new issues regarding either the isotopic composition of the munitions or the existence of another, heretofore unreported source of enriched uranium at the JPG site. (Alternatively, the ERMP sampling and analytical results are unreliable for their intended purpose, which is at least equally significant. In the third place, the fracture trace analysis shows that the FSP, as implemented, will be utterly and completely unable to perform its intended purpose at the JPG site. By themselves, each of these implications is significant; together, they are potentially profound. Additionally, they will require STV to retain and consult with at least one expert with very specialized expertise in the analysis and evaluation of isotopic uranium contamination, in addition to the three experts currently employed. *See* Norris Verified Statement, ¶ 22.

7. Based on the extensive experience of STV expert Charles H. Norris in such matters, it will require at least sixty (60) days beyond June 30, 2006, for STV's supplemented team of experts to assess properly the implications of the three new sources of information discussed above and formulate those implications into contentions and bases satisfying the format and content requirements of the applicable NRC rule. *See* Norris Verified Statement, ¶ 23.

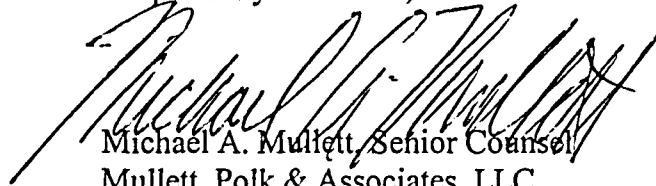
8. STV understands and accepts that the additional contentions and/or bases which it is requesting leave to file within sixty (60) days will be subject to objection by the Army and the NRC

Staff and rejection by the Board for failure to meet the substantive requirements of 10 C.F.R. § 2.309(f). By this motion, STV simply seeks to establish with certainty the time available to it to formulate and file the additional contentions and/or bases and thereby avoid a later controversy as to whether its filing is timely.

9. Counsel for STV certifies that he has reviewed this motion with counsel for the Army and the NRC Staff prior to filing. The Army's view is that the matters for which STV seeks leave to later file supplemental contentions and bases would not be relevant or material to the current proceeding. The Staff cannot agree, at this time, to the STV motion and thus plans to file a timely response in opposition to it.

WHEREFORE Petitioner STV respectfully requests leave to further supplement within sixty (60) days, pursuant to 10 C.F.R. § 2.309(f), its contentions and/or bases for hearing, as initially filed in this matter on November 23, 2005 ("Initial Contentions") and subsequently modified on May 31 2006 ("Final Contentions"), to address the significant implications of the three new sources of information discussed above which only recently became available to STV, as well as all other relief just and proper under the circumstances.

Respectfully submitted,



Michael A. Mullett, Senior Counsel
Mullett, Polk & Associates, LLC
309 West Washington Street, Suite 233
Indianapolis, IN 46204
Phone: (317) 636-5165
Fax: (317) 636-5435
E-mail: mmullett@mullettlaw.com

Attorney for Save the Valley, Inc.

UNITED STATES OF AMERICA
NUCLEAR REGULATORY COMMISSION
ATOMIC SAFETY AND LICENSING BOARD

Before Administrative Judges:

Alan S. Rosenthal, Chairman
Dr. Paul B. Abramson
Dr. Richard F. Cole

_____)	
In the Matter of)	Docket No. 40-8838-MLA
U.S. ARMY)	ASLBP No. 00-776-04-MLA
(Jefferson Proving Ground Site))	June 30, 2006
_____)	

VERIFIED STATEMENT OF CHARLES H. NORRIS

I, Charles H. Norris, state as follows:

1. I am a natural person over the age of eighteen years. I reside at 1928 E. 14th Avenue, Denver CO 80206.

2. I hold a Bachelor of Science degree with High Honors and Distinction in Geology, which I received from the University of Illinois in 1969. I hold a Master of Science degree in Geology, which I received from the University of Washington in 1970, where I was a National Science Foundation Fellow. I completed the required course work and passed the preliminary examination for a Ph.D. degree in geology at the University of Illinois in 1992, but I have not submitted or defended a thesis.

3. I have worked professionally as a geologist and hydrogeologist since 1972. I am a Principal (geology and hydrogeology) and President of Geo-Hydro, Inc., located in Denver,

Colorado. I am a licensed professional geologist in six states, including Indiana. I hold Indiana Professional Geologist License number 2100, which expires October 31, 2008. My areas of specialization include geology, hydrogeology, geochemistry, and the numerical techniques used in those areas. A copy of my resume has previously been submitted to the NRC as part of earlier filings.

4. I am retained by Save the Valley, Inc. (a) to review the application for changes to the NRC permit renewal for the Jefferson Proving Ground (JPG); (b) to review other technical materials related to the geology and hydrogeology in the area of, and adjacent to, JPG; (c) to assist with technical issues relating to any appeal by Save the Valley of changes to the permit; (d) to prepare explanatory materials to aid Save the Valley and its counsel in understanding technical issues relating to the significance of historic and contemporary monitoring at JPG; (e) to recommend modifications to the changes in the permit to ensure monitoring under the permit can be protective of public health and safety and of the environment; (f) to develop and prepare trial exhibits for admitted contentions and bases at any appeal hearing; (g) to prepare expert testimony for presentation or submission at any appeal hearing; and (h) if required, to attend and testify on behalf of Save the Valley at any appeal hearing.

5. As part of tasks (d) and (e) above, I have reviewed three sources of information and/or data which have become available to me only in the last three (3) weeks. Specifically, the information/data are (1) the Results of the October 2005 Environmental Radiation Monitoring Program (ERMP) Sampling Event, recently released to the ADAMS data base (ML061430302), (2) the Fracture Trace Analysis (SAIC, June, 2006), also recently released to the ADAMS data base (ML061670091), and (3) a research paper recently published by V. H. Coryell and D. M. Streams, "Molecular analysis of hprt mutations generated in Chinese Hamster Ovary EM9 cells

by uranyl acetate, by hydrogen peroxide and spontaneously” (Molec. Carcinogen. 2006. 45:60-72). Each of these sources, when evaluated in context with other existing information available from JPG and/or earlier scientific literature, materially impacts the understanding of the JPG facility with respect to the issues related to depleted uranium (DU) on the site, the migration of uranium from the site, the ability of the field sampling plan, as it is being implemented, to accomplish its objectives with respect to the migrating uranium, and the biological risks associated with the migrating uranium.

6. The October 2005 environmental radiation monitoring report shows results, which are confirmed by re-evaluation of the available environmental radiation monitoring reports from 2003 onward, that indicate either (a) the monitoring data that are being reported are inherently unreliable or (b) the nature of uranium contamination in and around the designated DU impact area at JPG is far more complex than previously realized and involves as yet unrecognized source(s) of uranium.

7. The report evaluates the data for evidence of DU from two parameters, the U238:U234 activity ratio and the weight percent of U235. The first parameter indicates DU is present if the ratio is (significantly) above a value of between 0.9 and 1.0, the ratio that is expected for natural uranium. The second parameter indicates DU is present (by regulatory definition) if the concentration of U235, expressed as weight percent, is less than 0.711, the value that is indicative of natural uranium. The report does not discuss the frequent occurrences in the data of U238:U234 activity ratios substantially below the 0.9 – 1.0 natural range and U235 concentrations substantially above 0.711 weight percent, characteristic of natural uranium. For example, monitoring well MW11 has an activity ratio of < 0.407 and a U235 concentration of < 14.3 weight percent. An examination of the previous year’s data, December 2004, confirms the

general magnitude of these values; the activity ratio then was 0.447 and the U235 concentration was 10.2 weight percent. These values are indicative of enriched uranium, not natural uranium or depleted uranium.

8. If JPG and the DU impact area contain only natural uranium and depleted uranium, the observed lower values of the activity ratios and the observed upper values of the U235 concentrations necessarily represent inaccurate and/or imprecise measurements of the uranium isotopes. If, due to precision or accuracy limits of the analytical data, the lowest values of the activity ratios and the highest U235 concentrations represent natural uranium, then the criteria for identifying DU, relative to these values, need to be re-scaled to the range that is reported, rather than the range that is normally expected. Such re-scaling would lead to the identification of DU where it is not presently acknowledged. However, since these anomalous values exist at multiple places, exist in multiple media, and persist over multiple sampling events, it is very unlikely that the problem of these unexpected values is just a reporting or laboratory error of some type.

9. Alternatively, if the isotopic data are valid as reported, they indicate the existence of enriched uranium in addition to natural uranium and DU on the JPG. None of the documents reviewed to date have described the existence of, or a potential source of, enriched uranium at JPG or in the DU impact area. A corollary of enriched uranium being present is that an isotope signature indicative of natural uranium could, as well, represent a mix of enriched uranium and DU, further complicating the interpretation of the monitoring data. Thus, if the data are accurate, and there is a source of enriched uranium at JPG, the Army's ERM program and the NRC Staff's EA must be modified to include its evaluation.

10. The October 2005 isotope data, accepted as reported, confirm earlier monitoring data

showing that DU exists in the impact area and does migrate. October 2005 data indicate that DU has migrated beyond the impact area and is found at the site boundary of the JPG. Monitoring point SD-/SW-2 is where Big Creek crosses the western boundary of the JPG. In October of 2005, the surface water draining from the JPG site had a U238:U234 ratio that was greater than 1.205 (sample) and less than 2.926 (duplicate), a ratio indicative of DU. Surface water at this point the previous fall showed a ratio that was characteristic of natural uranium. The Big Creek stream sediments at the western JPG site boundary show U238:U234 ratios indicative of DU in the October 2005 sample, as well as the spring and fall 2004 samples (1.255, 1.658, and 1.261, respectively). Only the duplicate sample for October 2005 was in the range of natural uranium (0.935).

11. The results of the fracture trace analysis that was implemented as part of the Field Sampling Plan were reported in June, 2006 (NRC ADAMS document number ML061670091), and based upon those results, the locations for lines for the electrical imaging (EI) survey were defined. The fracture trace analysis is the first step of a sequence of tasks that is to identify the optimal locations for nests of monitoring wells. The conceptual approach is that major fractures in geologic materials may correspond to enhanced conduits for groundwater flow. Some major fractures may manifest themselves as visible, linear features, or lineaments, on remote imaging media, such as air photos or satellite data. Mapping lineaments on appropriate media identifies possible fracture traces. Field verification (sometimes called "truthing"), which is part of the fracture trace analysis program per the Field Sampling Plan, helps distinguish between lineaments that may be related to major fractures and those that are not. To appreciate the inherent limitations of this methodology, one must understand that not all fractures express themselves with a visible lineament. Not all lineaments are fracture traces. Not all fracture

traces correspond to groundwater conduits. Not all groundwater conduits have an expression as a visible lineament. As designed for the Field Sampling Program, the follow-on EI survey is intended to refine the location of the verified fracture traces at depth and identify those likeliest to be groundwater conduits. The EI survey is not designated for use at JPG as a technique to be used independently of the fracture trace analysis.

12. Choosing optimal locations for monitoring wells using the steps laid out in the Field Sampling Plan is sequentially contingent upon successful completion of the following independent elements: a site with geologic characteristics capable of generating visible expressions of fracture traces, an imaging medium capable of capturing the visible expressions (lineaments) of fracture traces, accurate and precise identification of all lineaments on the imaging medium, accurate and precise transfer of lineaments from the imaging medium to accurate site maps, field verification of lineaments that are representative of fracture traces, and positioning of EI lines to refine fracture trace locations (including depth) and distinguish those with characteristics of groundwater flow. The report for the Fracture Trace Analysis indicates that there were substantial problems with each of these elements and none may have been successfully completed. The result is that choosing optimal locations for the nests of monitoring wells cannot be made by building upon the results of the fracture trace analysis as it has been performed.

13. Certification 4, the Contractor Statement of Independent Technical Review, states that significant concerns are documented in the project files. The report does not describe the significant concerns of the independent reviewer, it does not describe the resolution of the concerns, and it does not indicate what it means that, “. . . all concerns resulting from independent technical review of the project have been considered.” The project file should be

made available for review of these concerns.

14. The site characteristics and/or the imaging medium resulted in lineament expression that was poorer than other karst areas within the experience of the analyst. As stated on page 3-1, the mapped lineaments were ranked from "faint" to only "moderately distinct" and were "generally less distinct" than the other karst areas familiar to this analyst. Since the air photos were made in November, vegetative cover was unlikely the cause of the indistinct lineaments.

15. The Field Sampling Plan called for a site visit to verify the results of the photo analysis. This is a critical element for this type of study. It allows the identification of fracture traces to be distinguished from other possible causes of lineaments. It also allows the location of lineaments to be more precisely refined with respect to features that were not visible to the photo analyst. For example, a geologist in the field could refine the position of a mapped lineament in a karst area, like JPG, by noting the locations of cave mouths, spring discharges, and/or sink holes. There is no indication in the fracture trace analysis report that the needed field verification was ever performed. There are no discussions of the results of such a visit or description of refinements that were generated by such a field visit. All of the 110 photo-identified lineaments are reportedly shown on Figure 1, page 3-2 of the report, further reflecting no refinement by a field geologist.

16. The SAIC report acknowledges the choice of imaging medium created problems transferring the marked lineaments from the photos to contemporary maps. By choosing to use vintage air photos (1937) for the lineament study, in order to examine the site pre-JPG, there was a "paucity of useful features" to overcome photo distortion and registration problems and allow accurate and precise positioning of the individual lineaments on contemporary maps. The authors state that accuracy of placement on the contemporary map is estimated as

“approximately +/- 100 feet.” The impact of this acknowledgment is that even the best lineaments, ones that are “moderately distinct” on the air photo, are 200-foot wide bands when one is trying to locate them on contemporary maps. This imprecision is not conveyed in the lineament mapping that is represented on Figure 2 of the report, where lines representing the estimated location of the lineaments are thin and suggest precise locations.

17. The fracture trace analysis does not mention another inherent limitation of its methodology as implemented. By analyzing the photos only for linear features, one is analyzing only for vertical fractures. Fractures occur with orientations from vertical to horizontal. Fractures that are not vertical will not have linear fracture traces across land that has variable topography, such as is present at JPG. They will have curving traces. This has an important implication in the attempt to identify groundwater conduits. Major karst features often develop along flat or gently dipping intersection of major fractures. Such intersections do not result from the intersection of vertical fractures; the intersections of vertical fractures are always vertical. Thus, by limiting the trace analysis to linear traces, one is precluding an analysis of the most probable geologic control for major groundwater conduits.

18. The results of the fracture trace analysis clearly show the analysis is inaccurate and incomplete. As described in the cited reference in the first paragraph of Section 3 of the report, page 3-1, the analyst is identifying a “. . . natural linear feature consisting of topographic (including straight stream segments), vegetal, and soil tonal alignments” that extend less than one mile. Using the cited protocol, at a minimum the analyst should have identified and properly located all straight stream segments shorter than a mile in the mapped areas. They would have existed on the 1937 air photo and would still exist on a contemporary map, allowing accurate and precise registration and adjustment for distortion. This is demonstrably not the case,

however. Several examples are readily available from a quick examination of Figure 2 on page 3-3, the detailed area of the DU impact area. Section 4 marks the northern end of the impact area. There is a straight-line stream segment entering Section 4 almost north-south, approximately through the center of the northeast quarter of the section. This stream segment should have been analyzed as a lineament according to SAIC's cited reference, and it wasn't. The next two segments of this stream are approximated by mapped lineaments, but the locations and orientations should have been improved. By tying readily matching linear features, like streams, to a contemporary map, other non-matching features from the photos would be better positioned and oriented. Another example is found at the very southeast corner of Section 16, near the south end of the DU impact area. Here is another straight-line stream segment with no mapped lineament. There is a lineament shown in the same area that is oriented obliquely to the stream. If this lineament is the representation of the stream from the air photo, there remain registration and rotational errors that must be corrected before anything can be done with the map.

19. Only when a complete and accurate lineament map has been made, the features are tied to contemporary maps using unambiguous features such as stream segments and bends, and the lineaments are field verified, can a proper EI survey be defined. Since the Field Sampling Plan does not allow EI to be used to identify conduits that are not previously identified with a trace analysis, EI surveys in areas without identified lineaments do not contribute to the project and are wasted time and effort. The budgeted length of the EI program should be devoted to refining the position of traces that are possible conduits, not running down roads through areas where there are no such traces. Further, by restricting the EI traverses to north-south and east-west roads, it is impossible to orthogonally cross the traces that have been mapped in and around

the impact area. By restricting the EI traverses to the roads, the survey lines will necessarily approach and cross the potential fracture traces obliquely. The resolution of an EI traverse in refining the location of a conduit it crosses is best when the traverse is oriented normal to the feature. As the approach becomes more oblique, the signal is smeared and resolution is lost. To be effective, the EI program should consist of short traverses that are oriented normal to the anticipated groundwater conduits, with the total footage of the program used to cross the anticipated conduit multiply at regular intervals. As laid out, with the traverses simply following roads that are oblique to the features to be mapped and with much of the survey over country without mapped lineaments, the program will not contribute meaningfully to the successful identification of drilling locations that are needed to allow proper site characterization.

20. The recently published research by Coryell and Stearns (2006, as cited above) demonstrates a previously unidentified risk from uranium that would include DU. That research builds upon the earlier work by Stearns, *et al.* (Stearns DM, Yazzie M., Bradley AS, Coryell VH, Shelley JT, Ashby A, Asplund CS, Lantz RC. Uranyl acetate induces hprt mutations and uranium DNA-adducts in Chinese Hamster Ovary EM9 cells. *Mutagenesis* 2005 20:417-423), and Yazzie, *et al.* (Yazzie M, Gamble SL, Civitello ER, Stearns DM. Uranyl acetate causes DNA single strand breaks in vitro in the presence of ascorbate (Vitamin C). *Chem Res Toxicol.* 2003 16:524-530). It shows uranium to be a chemical mutagen. Previously, uranium was recognized as a radiological mutagen and a toxic metal, particularly for kidney damage. However, neither the exposure limits for uranium nor the risks from uranium assessed to potential receptors recognized the additional mutagenic risks associated chemically with uranium.

21. In short, the October 2005 ERMP results, if analytically reliable, show that depleted uranium has migrated to the JPG site boundary in at least two media and that a previously

unidentified source or sources of enriched uranium is present at the JPG site. The recent Coryell and Stearns research demonstrates a previously unidentified and unevaluated risk to human health and the environment at JPG. The fracture trace analysis report, central to the FSP approach for characterization of the JPG site, was not performed as proposed in the FSP, and thus cannot achieve the purpose it was intended to serve in the Army's site characterization approach. Together, these three new sources of information, when evaluated in context with other existing information available from JPG and/or earlier scientific literature, materially impact the understanding of the JPG facility. They impact the understanding of the risks to human health and the environment with respect to depleted (and other) uranium on the JPG site, the migration of uranium from the site, and the biological risks associated with the migrating uranium. They also impact the ability of the field sampling plan, as it is designed and is being implemented, to accomplish its objectives with respect to the migrating uranium and the biological risks associated with the migrating uranium.

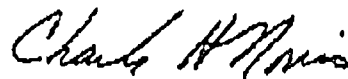
22. Given the short period of time since STV received these new sources of information, it has simply not been feasible to assess all of their implications for the characterization of the JPG site and then formulate those implications in contentions and bases meeting the format and content requirements of the NRC rules by June 30, 2006. But, there is no doubt that these implications are quite significant. In the first place, the evidence of DU at the JPG site boundaries raises significant issues regarding the need for environmental radiation monitoring and field sampling outside the JPG site boundaries. In the second place, the evidence of enriched uranium within the JPG site boundaries poses significant new issues regarding either the isotopic composition of the munitions or the existence of another, heretofore unreported source of enriched uranium at the JPG site. (Alternatively, the ERMP sampling and analytical

protocols and results are unreliable for their intended purpose, which is at least equally significant.) In the third place, the fracture trace analysis shows that the FSP, as implemented, will be utterly and completely unable to perform its intended purpose at the JPG site. Finally, new research indicates an entirely unevaluated biological risk associated with uranium that is supplemental to recognized biological risks. By themselves, each of these implications is significant; together, they are potentially profound. Additionally, they will require STV to retain and consult with at least one expert with very specialized expertise in the analysis and evaluation of isotopic uranium contamination in addition to the three experts currently employed.

23. Based on my past experience in such matters, it is my professional opinion that it would require at least sixty (60) days beyond June 30, 2006, for STV's supplemented team of experts to assess properly the implications of the three new sources of information discussed above and formulate those implications into contentions and bases satisfying the format and content requirements of the applicable NRC rule.

VERIFICATION

I, Charles H. Norris, hereby affirm under the penalty for perjury that the foregoing statements are true and accurate to the best of my knowledge, information, and belief.



Dated: June 29, 2006

Charles H. Norris, P. G.
Indiana Professional Geologist
License Number 2100
Expires 31-Oct-08

Molecular Analysis of *hprt* Mutations Generated in Chinese Hamster Ovary EM9 Cells by Uranyl Acetate, by Hydrogen Peroxide, and Spontaneously

Virginia H. Coryell and Diane M. Stearns*

Department of Chemistry and Biochemistry, Northern Arizona University, Flagstaff, Arizona

Naturally occurring uranium and depleted uranium (DU) are believed to be health hazards by virtue of both their chemical and radiological properties. The mechanism(s) behind uranium's chemotoxic effects has yet to be elucidated. Previous work has shown that DU, as uranyl acetate (UA), was mutagenic at the hypoxanthine (guanine) phosphoribosyltransferase (*hprt*) locus in XRCC1-deficient CHO EM9 cells. The purpose of the current study was to characterize the mutations induced by UA at the *hprt* locus of CHO EM9 cells and compare the mutation spectrum of UA with those of hydrogen peroxide and spontaneous mutations in the same line. The hypothesis being tested was that if DU as UA is chemically genotoxic then the mutation spectrum induced by the heavy metal should be distinct from that produced spontaneously or by H₂O₂. A total of 59 UA-induced, 38 spontaneous, and 45 H₂O₂-induced mutations were identified. Base substitutions comprised 29%, 42%, and 16% of UA, spontaneous, and H₂O₂ mutants, respectively. The frequency of G → T or C → A substitutions was not significantly different in spontaneous or H₂O₂-induced mutants than in UA-induced mutants, suggesting a possible role for 8-oxodG damage in UA mutagenesis. However, the observation that UA produced significantly more major genomic rearrangements (multiexon insertions and deletions) than occurred spontaneously suggests the possibility that DNA strand breaks or crosslinks could also be UA-induced mutagenic lesions. The unique mutation spectrum elicited by exposure to UA suggests that UA generates mutations in ways that are different from spontaneous and free radical as well as radiological mechanisms. © 2005 Wiley-Liss, Inc.

Key words: uranium; *hprt*; Chinese hamster ovary; hydrogen peroxide; DNA mutational analysis

INTRODUCTION

Uranium is a heavy metal that is both radiologically and chemically toxic. Its three major isotopes, U-238, U-235, and U-234, are radioactive, decaying by alpha, beta, and gamma emission with half lives on the geological time scale of 10⁹–10⁵ yr. Depleted uranium (DU) is uranium from which ~50–70% of the fissionable U-235 isotope has been extracted, and is thus ~40% less radioactive than natural uranium [1]. The most stable soluble form of uranium under physiological conditions is the uranyl cation, UO₂²⁺, in which uranium exists in the 6+ oxidation state. As a heavy metal, uranium can coordinate to biological molecules to exert a chemical toxicity.

Humans are exposed to uranium occupationally, and in the environment largely as a result of its occupational uses. Over half of the US uranium reserves are believed to exist on Native American lands [2], most significantly in and around the Navajo Indian Reservation in the Colorado Plateau region of Arizona, New Mexico, Colorado, and Utah. The intense mining effort of 1947–1971 resulted in uranium exposures in miners, mill workers, and ore transporters, and the US government has recently

acknowledged the harm performed by these exposures through the 1990 Radiation Exposure Compensation Act [3]. Environmental exposure to uranium continues to exist in these areas today as a result of abandoned mines and contaminated soil and water.

The depleted form of uranium is currently used by the military for anti-tank weapons, tank armor, and ammunition rounds because of the metal's high density and pyrophoric properties. The form of uranium used in weaponry is metallic; however, uranium(VI)/uranium(IV) oxides such as U₃O₇,

Abbreviations: DU, depleted uranium; UA, uranyl acetate; *hprt*, hypoxanthine (guanine) phosphoribosyltransferase; CHO, Chinese hamster ovary; αMEM, minimal essential medium eagle alpha modification; 6-TG, 6-thioguanine; 6-TG^r, 6-TG-resistant; RT-PCR, reverse-transcription polymerase chain reaction; *ef-2*, elongation factor 2 gene; UTR, untranslated region; ROS, reactive oxygen species; 8-oxodG, 8-oxo-2-deoxyguanosine.

*Correspondence to: Department of Chemistry and Biochemistry, Northern Arizona University, P.O. 5698, Flagstaff, AZ 86011-5698.

Received 28 January 2005; Accepted 6 September 2005

DOI 10.1002/mc.20155

U₃O₈, and UO₂, are formed upon burning [4], and solubilization of metallic uranium [4-6] is believed to produce uranyl cation *in vivo*. Estimates suggest that over 300 tons of DU were released into the environment during Gulf War I [7]. Estimates for Gulf War II are not yet available. Military personnel have been exposed to DU through inhalation of aerosolized particles or from shrapnel embedded in the skin. Monitoring of Gulf War veterans is in progress in the United States [6,8-15], Canada [16,17], and the United Kingdom [18]. Civilians' environmental exposure to DU may be less important than military exposures because residual uranium concentrations in the soil of the Persian Gulf region have not been found to exceed world-wide averages [19]. Occupational and environmental exposures to uranium have been linked to a variety of adverse health effects, with mining exposures better characterized than military exposures.

The health risks from occupational and environmental exposures to uranium mining have been found to include cancer, and possibly chromosomal aberrations and birth defects. Most of the epidemiological data on uranium mining has come from studies of the Navajo miners and of people exposed to mine tailings. The miners had well-established high incidences of lung cancer because of the absence of occupational safety requirements during the decades of heaviest mining activity [20-25]. However, data are not limited to the miners. In 1972, a study of cancer mortality found increases in prostate, pancreas, stomach, and colon cancer in men living on uranium mine tailings in Colorado relative to nearby populations not exposed to tailings; however, no increases in lung cancers or leukemia were found, suggesting radiation exposure was not the cause [26]. More recently, significant increases in gastric cancer were reported for counties in New Mexico with high deposits of uranium and uranium tailings [27]. A weak link between birth defects, stillbirths, and adverse outcomes of pregnancy was suggested for Navajo women living near uranium mine tailings [28]. A study of people exposed to tailings in Texas found a weak increase in chromosomal aberrations in lymphocytes of the exposed group relative to an unexposed group, and a significant increase in aberrations after lymphocyte challenge with gamma rays, indicating impaired DNA repair [29]. These studies imply that environmental exposure to uranium could target DNA or DNA repair pathways.

The possible risks from exposure to DU through military uses are more controversial than mining exposures. Allegations have been raised that there have been increased rates of lung, breast, bladder, skin, and stomach cancers and leukemia in Iraq after Gulf War I [30,31], and that other kidney and respiratory ailments are possible [32]; however, the World Health Organization has concluded that

thorough epidemiological studies have not yet been carried out [33]. There is no evidence yet supporting an increase in cancer rates in military personnel exposed to DU in the Balkans or the Persian Gulf [18,34-37] with the caveat that sufficient time may not yet have passed for final conclusions to be drawn.

Part of the difficulty of evaluating the health effects of uranium, natural or depleted, is that the different contributions of the metal's chemistry and radioactivity are not well understood. It is generally accepted that the greatest risk to uranium miners was the inhalation of radioactive radon-222, which is a gaseous decay product of U-238 that accumulated in the mine shafts. Radon is a well-established human lung carcinogen [38]; however, the risk from uranium exposure may not be limited to radon because the chemical genotoxicity of uranium has not been thoroughly evaluated.

We are interested in defining the extent to which uranium may be chemically genotoxic. Depleted uranium as uranyl acetate (UA) was previously found to produce DNA strand breaks *in vitro* in the presence of ascorbate [39], which suggests a chemical mechanism because the presence of ascorbate would not affect the half lives of uranium isotopes. Furthermore, UA was found to produce DNA strand breaks and uranium-DNA adducts and to be more mutagenic at the *hprt* locus of repair-deficient Chinese hamster ovary (CHO) EM9 cells than the parental CHO AA8 line, resulting in an average-induced mutation frequency (MF) of 31 per 10⁶ surviving cells, or an average eightfold increase in *hprt* mutants relative to untreated cells for a dose of 200 μ M UA over 24 h [40]. A separate study reported that alpha irradiation was no more mutagenic in the CHO EM9 line than the CHO AA8 line [41]; therefore, these opposing data suggest that uranium may have other mechanisms for damaging DNA than just radioactivity.

The purpose of the current study was to further explore the chemical genotoxicity of uranium by characterizing the mutations induced by UA at the *hprt* locus of CHO EM9 cells, and to compare the mutation spectrum of UA with that of H₂O₂ and spontaneous mutations in the same line, and with published reports of the mutation spectra of radon and alpha irradiation [42,43]. The hypothesis being tested was that if DU as UA is chemically genotoxic it would have a unique mutation spectrum distinct from those observed for spontaneous, free-radical, or alpha particle-induced mutations.

MATERIALS AND METHODS

Cell Culture and Mutant Isolation

CHO EM9 cells were obtained from the American Type Culture Collection (Manassas, VA). Cells were cultured in Minimal Essential Medium Eagle Alpha Modification (α MEM; Sigma Chemical Company,

St. Louis, MO) supplemented with 10% fetal bovine serum (Hyclone, Logan, UT), antibiotic (100 U/mL penicillin and 100 µg/mL streptomycin, Sigma), 250 ng/mL amphotericin B (Sigma), and 1 mM glutamine (Invitrogen-Gibco Life Sciences, Carlsbad, CA) at 37°C in humidified 5% CO₂/air.

Background mutations were eliminated by treating 3 × 10⁶ cells in a 150-cm² flask with supplemented αMEM and 200 µM hypoxanthine, 0.4 µM aminopterin, and 17.5 µM thymidine (HAT; Sigma) for 2 d. The cells were harvested, divided into 20–25 aliquots of 9 × 10⁵ cells in 100-mm dishes, and recovered for 3 d in supplemented αMEM with 200 µM hypoxanthine and 17.5 µM thymidine added.

Each dish was harvested, 8 × 10⁵ cells transferred to a new dish, allowed to adhere overnight, and treated with 200 µM UA (Spectrum Chemical Mfg. Corp., Gardena, CA) or 100 µM H₂O₂ (Sigma). After 24 h, 1 × 10⁶ cells from each dish were subcloned to 100-mm dishes. The cells were grown for 9 more days, subculturing 1 × 10⁶ cells every other day to maintain them in logarithmic growth and allow for mRNA and protein turnover. Spontaneous mutants were generated by growing 24 aliquots of 4 × 10⁵ HAT-treated and HT-recovered cells, as above, in 60-mm dishes for 4 wk, switching to 1 × 10⁶ cells in 100-mm dishes for 2 wk, and subculturing as necessary to avoid confluence.

Mutants resistant to 6-thioguanine (6-TG; Sigma) from each of the spontaneous, UA-treated, and H₂O₂-treated dishes were selected by subculturing 2.5 × 10⁵ cells in 100-mm dishes containing supplemented αMEM and 11 µg/mL 6-TG (6-TG-αMEM). After 10 d, up to four 6-TG-resistant (6-TG^r) clones per dish were transferred to individual wells of 96-well plates with 6-TG-αMEM. Each clone was expanded from 1 colony to 4–12 × 10⁶ cells in 6-TG-αMEM. The cells were harvested; 500-cell and 2 000 000-cell aliquots were delivered to each of five 0.2-mL PCR tubes (Fisher Scientific, Fair Lawn, NJ) and two 1.7-mL nuclease-free microcentrifuge tubes

(VWR International, West Chester, PA), respectively. All tubes were centrifuged for 5 min at 180g, the supernatant drawn off, and the tubes frozen at –80°C until use.

RT-PCR-PCR and cDNA Sequencing

The *hprt* mRNA of CHO EM9 clones was copied into cDNA and amplified in a single-tube reverse-transcription (RT)-polymerase chain reaction (PCR) reaction. A second PCR was performed with the RT-PCR reaction as DNA template. An "outer" pair of primers and nested "inner" primer pair (Table 1) were designed with PrimerSelect™ (DNASTAR, Madison, WI) and CHO mRNA sequences (GenBank Accessions J00060 [44] and X17656 [45]) to yield a 758 base-pair product. The primers for cDNA sequencing (Table 1) were designed with the same tools. All DNA oligomers were ordered from Integrated DNA Technologies, Inc., Coralville, IA.

The initial RT-PCR methods were a combination of the recommended protocol for Robust RT-PCR (Finnzymes Oy-MJ Research) and the published procedure of Yang and coworkers [46]. The Robust RT-PCR procedure (Finnzymes Oy-MJ Research, Waltham, MA) was used, but a frozen 500-cell aliquot was used to supply the mRNA template and Nonidet P40 was added to the RT-PCR reaction mixture. The reaction consisted of a 20-µL aliquot of 1 × Robust RT-PCR buffer (Finnzymes Oy-MJ Research), 1.5 mM MgCl₂, 200 µM each dNTP, 1 U/µL Prime RNase Inhibitor™ (Eppendorf, Hamburg, Germany), 0.1 U/µL avian myeloblastosis virus reverse transcriptase (AMV-RT; Fisher), 0.1% Nonidet P40 (Rosche, Mannheim, Germany), 200 nM primer Ao5, 200 nM primer Ao3, 0.04 U/µL DyNAzyme™ EXT DNA polymerase cocktail (Finnzymes Oy-MJ Research), which was added to a 0.2-mL PCR tube with an aliquot of 500-cells. A negative control of a tube with no cells was included along with a positive control of a 500-cell aliquot of wild-type EM9. Reverse transcription (RT) was carried out for 1 h at 50°C and was

Table 1. Primers Used to Copy and Amplify CHO EM9 *hprt* and *ef-2* mRNA, and Sequence CHO EM9 *hprt* cDNA

Primer name	Primer sequence (5' → 3') ^a	Primer function(s)
Ao5	cctcaccgcttctcgtg	5' <i>hprt</i> -specific RT-PCR
Ao3	cagatggctgcagaactagaatg	3' <i>hprt</i> -specific RT-PCR
Ai5	cctcctcacaccgctcttc	5' nested <i>hprt</i> -specific PCR and 5' cDNA sequencing
Ai3	actgggaacatgaatgggactc	3' nested <i>hprt</i> -specific PCR and 3' cDNA sequencing
As5a	GGGAGGCCATCACATTGT	Upstream 5' cDNA sequencing
As5b	GTTGAGGACATAATTGACACTGG	Downstream 5' cDNA sequencing
As3a	GATCATTACAGTAGCTCTTCAGTCT	Upstream 3' cDNA sequencing
As3b	TCTGGCCTATATCCAACACTTC	Downstream 3' cDNA sequencing
A2o5	ctATGGTGAACCTTCACGGTAGAC	5' <i>ef-2</i> -specific RT-PCR
A2o3	CAATGATGTGCTCCCCAGAC	3' <i>ef-2</i> -specific RT-PCR
A2i5	GTGTGCAAGGCGGGTATCA	5' nested <i>ef-2</i> -specific PCR
A2i3	CCGCCTCATCATCAGGTGG	3' nested <i>ef-2</i> -specific PCR

^aLower case letters designate 5' UTR, intron, or 3' UTR sequence and upper case letters designate exon sequence.

followed by 2 min at 94°C to denature the AMV-RT. The reactions were then subjected to 38 cycles of a denaturation step of 30 s at 94°C, an annealing step of 30 s at a 60.5°C, and a 2 min extension at 72°C. A final extension of 10 min at 72°C concluded the RT-PCR reaction. The heated lid was at 104°C during the procedure.

The second, nested, PCR contained 50 mM Tris-HCl (pH 9.0), 1.5 mM MgCl₂, 15 mM (NH₄)₂SO₄, 0.1% Triton X-100, 6.7% sucrose, 100 μM xylene cyanol, 300 μM each dNTP, 400 nM primer A15, 400 nM primer A13, 10% RT-PCR reaction as template, and 0.02 U/μL DyNAzyme™ EXT. Two negative controls were performed: one contained 10% of the RT-PCR reaction performed with no cells as the template and the second used 10% water as the template. The wild-type EM9 reaction provided the positive control. All nested-PCR reactions were denatured at 94°C for 2 min, then cycled 38 times with a denaturation of 30 s at 94°C, 30 s at 62°C for primer annealing, and an extension for 1 min at 72°C. A final extension of 10 min at 72°C concluded the PCR. During the PCR, the lid temperature was at 104°C. The fragments produced, or amplicons, were visualized on 1.5% agarose (Invitrogen) gels with 2% of each reaction.

Reactions that produced more than one band were reamplified at a higher temperature. Another aliquot of the original RT-PCR reaction was used as template for a second nested PCR (RT-PCR-PCR). The nested PCR conditions were the same as the first time, except the annealing temperature was raised to between 63.5 and 65.1°C. A 2% aliquot of each reaction was visualized on a 1.5% agarose gel.

All RT-PCR-PCR reactions yielding a single band were sequenced, including wild-type EM9. Single-amplicon reactions were purified with DNA Clean & Concentrator™-5 columns (Zymo Research, Orange, CA) and quantified. The purified DNAs were sequenced at the University of Arizona DNA Sequencing Service with an Applied Biosystems 3730XL DNA Analyzer and between two and six of the cDNA sequencing primers (Table 1), depending on the size of the fragment. The various sequences generated for each mutant were aligned with SeqMan™II (DNASTAR) and miscalls were corrected. Each mutant's consensus sequence was then compared to the wild-type EM9 consensus sequence with MegAlign™ (DNASTAR). Changes in the mutants' hprt cDNA sequences were tabulated.

Any RT-PCR-PCR reactions, not producing an amplicon, were repeated at more permissive temperatures. The complete RT-PCR-PCR procedure was repeated with a new 500-cell aliquot, with the only differences being that the RT was performed at 48°C and both of the PCR annealing temperatures were dropped to 59°C. Reactions still not producing an amplicon were multiplexed with the hprt primers and primers specific to CHO elongation factor 2 (ef-2) mRNA.

Multiplex RT-PCR-PCR

Multiplex RT-PCR-PCR was performed with primers specific for CHO hprt and ef-2 mRNA. The ef-2 primers (Table 1) were designed from CHO ef-2 sequence data (GenBank Accession J03200 [47]) to yield a 1,027 base-pair amplicon. Multiplex RT-PCRs were performed under the same conditions as the more permissive hprt RT-PCRs, except primers specific for ef-2 mRNA, A2o5, and A2o3 (Table 1), were each at 200 nM in the reaction as well as the hprt-specific primers Ao5 and Ao3. The second, nested, multiplex PCRs had the same conditions as the more permissive nested PCRs with the exception of the primers. The hprt-specific primers A15 and A13 were each at 300 nM and the ef-2-specific primers A2i5 and A2i3 (Table 1) were each at 425 nM. The reaction products were visualized on 1.5% agarose gels.

Genomic PCR

The hprt exons and flanking sequences were amplified with genomic DNA as template. Some genomic hprt primers (Table 2) were designed de novo from GenBank Accessions X53073, X53076, X53077, X53078, X53079, and X53080 [45] to better match primer annealing temperatures and place the primers so they included no exon sequence, with DNASTAR's PrimerSelect™, while others were obtained from the literature [45,48]. The ef-2 primers (Table 2) were designed with GenBank Accession J03200 [47]) and PrimerSelect™.

Wild-type CHO EM9 and mutant genomic DNA was isolated from 2 × 10⁶-cell aliquots with ZR Genomic DNA Kit™ columns (Zymo Res.) and quantified. All exon PCR reactions contained 50 mM Tris-HCl (pH 9.0), 15 mM (NH₄)₂SO₄, 0.1% Triton X-100, 6.7% sucrose, 100 μM xylene cyanol, 1.0 mM each dNTP, 5.0% DMSO, 0.05 U/μL DyNAzyme™ EXT DNA Polymerase (MJ Research, Waltham, MA), and 5 ng/μL genomic DNA as template. Exon 4 was amplified along with the ef-2 fragment at 5.5 mM MgCl₂, 1.5 μM of each exon 4 primer, and 0.07 μM each ef-2 primer (Table 2). The amplification was performed with the lid temperature at 104°C and consisted of an initial denaturation for 2 min at 94°C followed by 38 cycles of denaturation for 20 s at 94°C, primer annealing for 30 s at 59°C, and a 50 s extension at 72°C, and concluded with a final extension of 10 min at 72°C. A single multiplex reaction for the ef-2 fragment and exons 1, 2, and 6, and the amplicon containing exons 7 and 8, was performed with 6.0 mM MgCl₂, primers for the exons at appropriate concentrations, and 0.176 μM ef-2 primers (Table 2). The PCR program was identical to the exon 4 program. Exons 5, 9, and the ef-2 internal standard were multiplexed with 6.5 mM MgCl₂, exons' 5 and 9 primers at 3 μM, and 0.4 μM each, respectively, and 0.095 μM of each ef-2 primer (Table 2). The amplification program was the same

Table 2. Primers for Genomic PCR of *hprt* and *ef-2* loci, and Sequencing at the *hprt* Locus of CHO EM9

Primer name	Primer sequence (5' → 3') ^a	Primer use	Final concentration, μ M	Wild-type amplicon size, base pairs
AX1.5	cctcaccgctttctcgtg	5' <i>hprt</i> exon 1	0.12	361
AX1.3	gcctcacaagcagtcacc	3' <i>hprt</i> exon 1	0.12	
AX2.5 ^b	agcttatgctctgattgaaatcagctg	5' <i>hprt</i> exon 2	0.588	232
AX2.3 ^c	gaactcagaacctctggaagagc	3' <i>hprt</i> exon 2	0.588	
AX3.5 ^c	ggaactcgtctattccgtgatttta	5' <i>hprt</i> exon 3	2.0	273
AX3.3 ^c	tacatacaaaactaggattgcatatt	3' <i>hprt</i> exon 3	2.0	
AX4.5 ^c	tgtgtgtattcaagaatgcatg	5' <i>hprt</i> exon 4	1.5	177
AX4.3	gcacagttaactaattgattctgg	3' <i>hprt</i> exon 4	1.5	
AX5.5	ctgataattggaatatatctcacttc	5' <i>hprt</i> exon 5	3.0	150
AX5.3	cctggcttacctatagtatacac	3' <i>hprt</i> exon 5	3.0	
AX6.5	cttaccacttaccataaatacctcttttc	5' <i>hprt</i> exon 6	1.176	182
AX6.3	gcaattgcttattgctccaatg	3' <i>hprt</i> exon 6	1.176	
AX7.5	gttctattgctttcccatatgtcacatg	5' <i>hprt</i> exons 7/8	0.44	446 for a single amplicon with exons 7 and 8
AX8.3	ctggtcaaatgacgaggtgctag	3' <i>hprt</i> exons 7/8	0.44	
AX9.5 ^c	cctgtttgtaggaacagacaattc	5' <i>hprt</i> exon 9	0.4	403
AX9.3	caatctcagcatttttaatagtggt	3' <i>hprt</i> exon 9	0.4	
A2g5	gctacatagtagggactctgtc	5' <i>ef-2</i> genomic	0.07, 0.176, 0.095	861
A2g3	CAggtaggagctaaactaccg	3' <i>ef-2</i> genomic	0.07, 0.176, 0.095	

^aLower case letters designate 5' UTR, introns, or 3' UTR sequence and upper case letters designate exon sequence.

^b[45].

^c[48].

as that for the exon 4 multiplex, excepting the primer-annealing temperature was 57°C. Exon 3 was amplified alone with 5.5 mM MgCl₂ and 2 mM each exon 3 primer. The exon 3 program differed from exon 4's in that the primer annealing temperature was lowered to 45°C and the extension time shortened to 20 s. Amplification products for all reactions were visualized on 2.5% SynergelTM (Diversified Biotech, Boston, MA), 1% agarose gels. Amplification results were tabulated.

Genomic PCR and Sequencing of Individual Exons

Mutant genomic DNA was amplified by PCR, purified, quantified, and sequenced. The PCR reaction and amplification program conditions for exon 3 were the same as above. The other exons' conditions were the same as for the multiplex reactions in which they were amplified with the following modifications: the annealing temperature for exon 5 was lowered to 55.1°C and each of the primers for exon 1 was at 0.15 μ M, 0.6 μ M for exon 2, 2 μ M for exon 4, 1.2 μ M for exon 6, 0.6 μ M for exon 9, and 0.5 μ M for the amplicon containing exons 7 and 8. An aliquot of each reaction was visualized on a 2.5% SynergelTM, 1% agarose gel, while the remainder was purified with Zymo Research DNA Clean & ConcentratorTM-5 columns, and quantified. The DNA templates were sequenced in both directions with the appropriate primers (Table 2) by the University of Arizona DNA Sequencing Service. The sequences were aligned with SeqManTMII (DNASTAR), miscalls corrected, and compared to the corresponding CHO sequence [45] with MegAlign (DNASTAR). Mutations were tabulated.

Statistics

The significance of differences among the mutation spectra was determined by calculating both the R \times C contingency table, χ^2 -test [49], and the corresponding R \times C contingency table log-likelihood ratio test (G), which is suggested for data having at least one category with a small observed frequency [50]. Because our data did have small observed frequencies, the log-likelihood ratio test was used to determine the significance of the differences. When differences were significant, the tables were subdivided [49] to investigate the nature of the differences. The UA mutation spectrum was compared to those of α particles and radon by grouping the UA mutation categories into ones corresponding to those of Schwartz et al. [42] and Jostes et al. [43], respectively, and calculating G for the two comparisons. Differences were deemed significant at $P \leq 0.05$.

RESULTS

The purpose of this work was to generate and compare *hprt* mutations in base-excision-repair (BER) deficient CHO EM9 cells exposed to UA, H₂O₂, or generated spontaneously. Independent populations of CHO EM9 cells were passaged for 6 wk to accumulate spontaneous (S) mutations, and two groups of independent EM9 populations were exposed to either 200 μ M UA or 100 μ M hydrogen peroxide (H) for 24 h. There was an average of 43, 31, and 16 6-TG^r colonies per 10⁶ viable cells in the UA, H₂O₂, and untreated cells for four experiments with cells treated with 200 μ M UA and 100 μ M H₂O₂ for

24 h. The average-induced mutation frequency (the treated-untreated difference,) was 28 for UA and 15 for H₂O₂. The mutant increase above background (the ratio of treated to untreated) was 2.8 and 2.0 for UA and H₂O₂, respectively.

Up to four 6-TG^r clones were selected from each independent population in all three treatment groups. Clones of varying sizes were chosen based on the assumption that different phenotypes would represent different genotypes, thus providing a broader sampling of mutations. Clones from each independent population (100-mm dish) were given the same numeric designation, and each clone from a given population was labeled a, b, c, or d. For example, UA-treated mutants UA18 a, b, c, and d came from the same independent population while UA19 a, b, c, and d came from a different independent population. For molecular analysis at the *hprt* locus, 72, 56, and 47 clones from the UA, S, and H groups, respectively, were expanded. We characterized the mutations in 50, 36, and 25 clones from the UA, S, and H groups; the remaining clones were discarded as sibling clones from the same independent population or because of sequencing problems. We were unable to fully characterize one clone's mutation. The clones characterized yielded 59, 38, and 45 mutations for the UA, S, and H groups, respectively.

Characterization of the cDNA From 6-TG^r Clones

Wild-type and mutant EM9 *hprt* mRNA was reverse-transcribed (RT) and amplified by PCR in a single reaction mixture, and this was followed by a second PCR to generate sufficient quantities of cDNA for sequencing. These tandem reactions were performed on all expanded clones.

Of the total expanded mutants, the cDNAs of 71, 54, and 43 clones from the UA, S, and H groups, respectively, were sequenced. The remaining clones produced multiple amplicons and therefore were not sequenced. Of the mutants that were sequenced, the clones assumed to be sibling clones by virtue of having the same cDNA sequence as another clone from the same independent population were discarded.

The cDNA base substitutions, insertions, and deletions sequences identified from independent clones are found in Table 3. Nucleotide positions for the *hprt* cDNA are designated such that the A of the initial AUG codon is nucleotide 1 and the second A of the terminal TAA is base 657. The first and second nucleotides 5' to the initial AUG are designated -1 and -2, respectively; that numbering continues 3'-to-5'. Exon (coding) sequences are in upper case; 5' and 3' untranslated regions (UTR) and introns, all non-coding sequences, are in lower case. We sequenced both CHO AA8 and EM9 wild-type cDNAs and found them to be identical to the published coding sequence (GenBank Accession X59692 [51]).

The UA-generated mutants had 6 transitions, 7 transversions, and 8 insertions in their cDNAs (Table 3). Duplications of exon 5 and in exons 6-8 as a unit, were common. Two of the clones had G substituted for A at position 401 and four had a T substituted for G₂₃₈ (Table 3). One third of the UA-induced cDNA mutations were in exon 3, the largest exon and thus the largest single coding-region mutational target. Exon 3 also codes for the protein's active site, which would make it more likely that small mutations would result in the ablation of the protein's function.

The spontaneously generated mutants had 2 transitions, 11 transversions, 6 deletions, and 1 insertion in their cDNA sequences (Table 3). Of the 11 total transversions, 8 were G-to-T substitutions, and 7 of these were at G₂₃₈. There were also 4 different deletions, as well as an insertion of bases -8 through 282, at base 283 (Table 3). Of these mutations, 65% were in exon 3 which is again consistent with the expectation that an intact exon 3 is important to protein function.

Hydrogen peroxide exposure generated five independent 6-TG^r mutants whose changes were detected in their cDNA sequences (Table 3). Three of the five H₂O₂-induced cDNA mutants had deletions in exon 3, again reflecting the central role of exon 3 in HPRT function.

Multiplex RT-PCR-PCR

Multiplex RT-PCR-PCR reactions were carried out on mutants whose RT-PCR-PCR reactions produced no amplicon to verify that negative results were not because of reaction failures. The 10 UA, 5 S, and 10 H₂O₂ clones from independent populations not producing a cDNA amplicon, even with lowered annealing temperatures, were copied and amplified in multiplex reactions with primers specific to *ef-2* and *hprt* mRNAs (Table 2). The inclusion of *ef-2*-specific primers served as an internal positive control because the absence of an *hprt* band coupled with the presence of an *ef-2* band could be attributed to an *hprt*-specific failure and not to the failure of the PCR reaction. The wild-type EM9 multiplex reaction resulted in *ef-2* and *hprt* amplicons at 1,027 and 758 base pairs, respectively (Figure 1), demonstrating that the reaction produced the anticipated result when both *ef-2* and *hprt* mRNAs were intact. All of the clones so tested produced an *ef-2* amplicon but no *hprt* amplicon, demonstrating our negative results were not because of PCR reaction failures. We inferred that these mutants had mutated or missing *hprt* 5' and/or 3' UTR, which suggested the presence of genomic deletions or splice-sequence mutations involving at least the sequences flanking exons 1 and/or 9.

Genomic PCR

The genomic DNA was isolated from mutants whose cDNA sequences skipped one or more exons

Table 3. UA-induced (UA), Spontaneous (S), and H₂O₂-Induced (H) Mutations Observed in CHO EM9 *hprt* cDNA

Mutant(s)	Mutation	Exon	Predicted protein consequence
Base substitutions			
Transitions			
S5a	G ₂₀₉ → A	3	Gly ₇₀ (GGG) → Glu (GAG)
UA21d, UA22a	A ₄₀₁ → G	5	Glu ₁₃₄ (GAG) → Gly (GGG) Exon 5 donor site
UA22b	A ₄₂₇ → G	6	Met ₁₄₃ (ATG) → Ala (GTG)
UA10b	A ₄₃₃ → G	6	Thr ₁₄₅ (ACT) → Ala (GCT)
S4a	C ₅₀₈ → T	7	Arg ₁₇₀ (CGA) → stop (TGA)
UA23d	C ₅₅₁ → T	8	Pro ₁₈₄ (CCA) → Leu (CTA)
UA16c	T ₅₉₅ → C	8	Phe ₁₉₉ (TTC) → Leu (CTC)
H2a	G ₆₁₇ → A	9	Cys ₂₀₆ (TGT) → Tyr (TAT)
Transversions			
UA16d, S11d	A ₁₃₁ → T	2	Asp ₄₄ (GAC) → Val (GTC)
S9d	G ₁₉₀ → C	3	Ala ₆₄ (GCC) → Pro (CCC)
UA13a, S1c	C ₂₂₂ → A	3	Phe ₇₄ (TTC) → Leu (TTA)
UA23a, UA24c, UA25a, UA26, S1a, S3b, S6c, S9b, S10b, S11a, S12a	G ₂₃₈ → T	3	Asp ₈₀ (GAT) → Tyr (TAT)
UA19c	A ₄₀₉ → C	6	Ile ₁₃₇ (ATT) → Leu (CTT)
H18d	A ₄₂₄ → C	6	Thr ₁₄₂ (ACA) → Pro (CCA)
S8a	G ₆₀₆ → T	8	Leu ₂₀₂ (TTG) → Phe (TTT)
Deletions			
S14b, S16a	A ₈₃ T ₈₄	2	Tyr ₂₈ ...Arg ₄₅ Thr ₄₆ → Cys ₂₈ ...Asp ₄₅ Stop
H14b	G ₁₅₂	3	Arg ₅₁ Asp ₅₃ Val ₅₄ Met ₅₄ → Gln ₅₁ Met ₅₃ Ser ₅₃ Stop
H11a, H13c	164-170	3	Lys ₅₅ ...Leu ₆₅ Cys ₆₆ → Arg...Cys ₆₅ Stop
S2c, S3a	263-268	3	Ser ₈₉ , Asp ₉₀ deleted
S11b	A ₄₂₄	6	Thr ₁₄₂ ...Leu ₁₆₄ Val ₁₆₅ → Gln ₁₄₂ ...Trp ₁₆₄ Stop
S5b	T ₄₃₅ C ₄₃₆	6	Leu ₁₄₆ ... → Ala ₁₄₆ ...Gly ₁₅₉ Stop
Insertions			
UA10c	GA after A ₄₀₁	5	Asp ₁₃₅ Ile ₁₃₅ → Arg ₁₃₅ Thr ₁₃₅ Stop
UA6b	C after C ₄₆₅	5	Lys ₁₅₆ Met ₁₅₆ Val ₁₅₆ Lys → Gln ₁₅₆ Asn ₁₅₆ Gly ₁₅₆ Stop
UA9b	Exons 2-3 duplicated		
UA11a, UA12a, UA21c, UA20a, UA24b S15b	Exons 6-8 duplicated Bases -8 to 282 duplicated in cDNA sequence		

and from those that produced no *hprt* cDNA to determine if these changes resulted from genomic mutations. All nine exons could be amplified in a total of four PCR reactions. The relevant exons, except exon 3, were multiplexed with *ef-2*-specific genomic primers (Table 2) as an internal positive control, and visualized on 2.5% Synergel, 1% agarose gels. Gels of the wild-type products verified that the fragments were of the expected sizes (Figure 2). The amplification of both exons 3 and 4 produced artifacts (Figure 2B and D), but these did not appear to inhibit target amplification. Exon 3 was the only exon not able to be multiplexed with *ef-2* as an internal standard (Figure 2D); therefore, any negative results for exon 3 were repeated at least once more. However, in all cases for exon 3 amplifications, other samples amplified with the same exon 3 reaction mixture did produce bands, suggesting the

failures were not due to reaction failure but due to a lack of appropriate template flanking exon 3.

Thirteen UA, eight S, and six H mutants had genomic deletions that corresponded exactly to the skipped cDNA exons, suggesting that whole-exon genomic deletions were responsible for the skipping of those same exons in the cDNA sequences, rather than genomic splice-sequence mutations (Table 4). Single-exon deletions included exons 2, 4, 5, 7, and 8, while multiple-exon deletions encompassing exons 2-3, 2-4, and 4-5 were identified (Table 4).

In mutants UA8b, UA21a, and S6a, exons 2-4 were skipped in their cDNA sequences, but exon 4 amplified from their genomic DNAs (Table 4). Pleiotropic effects of intronic splice sequence mutations in introns 2 or 3 resulting in the loss of more than one exon have been documented for human *hprt* mutations [52], so it is possible that the loss of

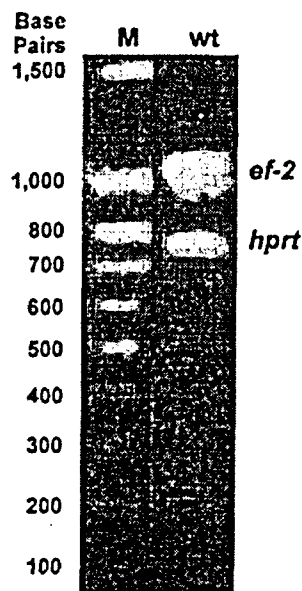


Figure 1. Multiplexed cDNA amplicons generated with primers specific for *elongation-factor 2* (*ef-2*) and *hprt* mRNAs of wild-type CHO EM9 cells (wt), as compared to a 100-base-pair ladder (M).

intron 2 and 3 splicing sequences, rather than the genomic loss of exon 2 and/or 3, was responsible for the additional exons skipped in the cDNA sequences from these mutants.

Three mutants had fewer exons skipped in their cDNA sequences than genomic failures (H9d, H17a, and H10b, Table 4). Exon 1 or 9 was the additional genomic exon not amplified in these cases. Primer AX1.3 (Table 2) starts some 247 bases downstream of the 3' end of exon 1 while primer AX9.5 (Table 2) begins 90 bases 5' of the start of exon 9, so it is

possible that those primer sites were deleted, but the splicing sequences remained intact for the proper splicing of exons 1 and 9, respectively.

The mutants from which no cDNA could be amplified had a variety of genomic PCR failure patterns. Losses including exon 1 (UA14a, UA16b, S6d, S9a, S11c, S13b, H13d, H17b, Table 4) may have resulted in the loss of the promoter site for transcription, resulting in no pre-mRNA production. Losses encompassing exon 9 (UA9a, H5b, Table 4) may have included the loss of the polyadenylation signal(s), resulting in improper pre-mRNA processing and no mature mRNA production. Genomic PCR produced no *hprt* amplicons at all in five UA, one S, and two H₂O₂ mutants (UA4b, UA7a, UA13c, UA17a, UA21b, S15a, H9b, H19b, Table 4), suggesting whole-gene deletions were responsible for their cDNA amplification failures.

Mutants whose skipped cDNA exons were successfully amplified from their genomic DNAs were inferred to be splice-sequence mutations rather than whole-exon deletions.

Genomic Amplicon Sequences

The relevant exons of suspected splice-sequence mutants were re-amplified and sequenced for further characterization. Each exon and flanking intronic sequence was amplified alone with the appropriate genomic PCR primers (Table 2). The amplicons were purified and sequenced in both directions with the amplification primers. One UA and one S clone produced poor sequence and were discarded. No changes were seen in the sequences of exons 2, 3, or 4 for clone H7b (Table 5), indicating that we had not successfully characterized the genomic mutation responsible for skipping those exons in the cDNA; it was therefore removed from our analysis. Although sequencing of the H13a exon 4 amplicon produced

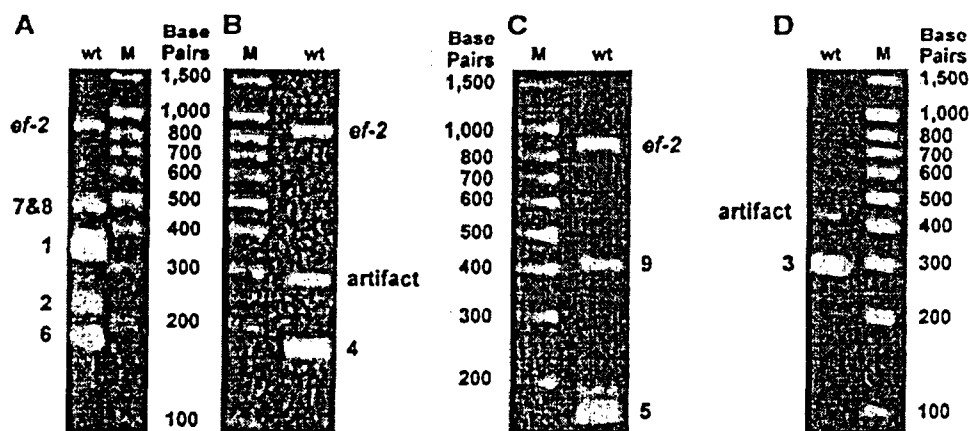


Figure 2. Amplification of CHO EM9 genomic DNA. Multiplex reactions of (A) *ef-2* genomic fragment and *hprt* exons 7 and 8 together, exon 1, 2, and 6, (B) *ef-2* genomic fragment and *hprt* exon 4, (C) *ef-2* genomic fragment and *hprt* exons 5 and 9. PCR reaction (D) of exon 3. All wild-type EM9 (wt) fragment sizes were compared to a 100-base-pair ladder (M).

Table 4. UA-Induced (UA), Spontaneous, and H₂O₂-Induced (H) *hprt* Mutants With Genomic Exon Deletions

Mutant(s)	Exon(s) that did not amplify	cDNA phenotype
S6d, S9a, S13b	1	No cDNA amplified
UA3b, UA11b, UA17b, S13c, S17c	2	Exon 2 skipped
UA8b, S6a	3	Exons 2-4 skipped
UA12b, UA20b, S16c, S17a, H9c	4	Exon 4 skipped
UA10a, UA11d, S7a, H12c	5	Exon 5 skipped
UA18a, S1d	No 7/8 amplicon	Exons 7-8 skipped
H5b	9	No cDNA amplified
UA16b	1-3	No cDNA amplified
H9d, H17a	1-4	Exons 2-4 skipped
UA14a, S11c, H13d, H17b	1-4	No cDNA amplified
UA4b, UA7a, UA13c, UA17a, UA21b, S15a, H9b, H19b	1-9	No cDNA amplified
UA5a, UA12c, S2a, H1b, H16a, H19a	2-3	Exons 2-3 skipped
UA21a	2-3	Exons 2-4 skipped
UA11c, UA15c, H15a	2-4	Exons 2-4 skipped
H10b	2-9	Exons 2-8 skipped
UA19a	4-5	Exons 4-5 skipped
UA9a	6-9	No cDNA amplified

unusable sequences, it was evident from the agarose gel that approximately 22 bases were deleted from the amplicon (Figure 3). Because there are 24 and 39 bases from the 66-base exon 4 to primers AX4.5 and AX4.3, respectively, it was inferred that the 22-base deletion in H13a encompassed one of the splice sites, resulting in the absence of exon 4 from the cDNA sequence.

Clones UA1b, UA8b, UA19b, and S14a had the same transversion: t was substituted for the g 30 nucleotides 5' of exon 2 (Table 5). In UA19b and S14a, this resulted in skipping exon 2 in the cDNA. For mutants UA1b and UA8b, however, exons 2 to 4

were skipped in the cDNA sequence; this may be because of the pleiotropic effects possible with perturbations in exon 2 [52].

Three clones (UA22d, S10d, S19, Table 5) had two intronic mutations each. In each case, a change was identified at or near an affected exon splice site, with the second mutation occurring a greater distance from the exon. For seven clones (UA2a, UA24a, H3a, H4a, H6a, H7c, and H16b, Table 5), no cDNA was produced, and each mutant had the same five mutations. Three of the mutations were 5' of exon 9, one was 3' of exon 9, and the last was 3' of

Table 5. UA-Induced (UA), Spontaneous (S), and H₂O₂-induced (H) *hprt* Intronic Deletion Mutants

Mutant	Genomic DNA mutation ^a	cDNA phenotype
Base substitutions		
Transitions		
S10d	Intron 4: g _{[exon5]-1} → a; loss of exon 5 splice site	Exon 5 skipped
S19	Intron 7: g _{[exon8]-1} → a; loss of exon 8 splice site	Exon 8 skipped
Transversions		
UA19b	Intron 1: g _{[exon 2]-30} → t	Exon 2 skipped
UA1b, UA8b, S14a	Intron 1: g _{[exon 2]-30} → t	Exons 2-4 skipped
UA2a, UA24a, H3a, H4a, H6a, H7c, H16b	Intron 8: a _{[exon 9]-76} → t	No cDNA amplified
Deletions		
H13a	≈ 22 bp from exon 4 amplicon	Exon 4 skipped
S10d	Intron 5: c _{[exon 5]+42}	Exon 5 skipped
UA2a, UA24a, H3a, H4a, H6a, H7c, H16b	Intron 8: c _{[exon 9]-18}	No cDNA amplified
UA22d	Intron 8: g _{[exon 8]+51a+a+8}	Exon 8 skipped
Insertions		
UA2a, UA24a, H3a, H4a, H6a, H7c, H16b	Intron 1: g after g _{[exon 1]+29}	No cDNA amplified
UA22d, S19	Intron 7: g after g _{[exon 7]+19}	Exon 8 skipped
UA2a, UA24a, H3a, H4a, H6a, H7c, H16b	Intron 8: c after c _{[exon 9]-42}	No cDNA amplified
UA2a, UA24a, H3a, H4a, H6a, H7c, H16b	3' UTR: t after t _{[exon 9]+180}	No cDNA amplified
Not characterized		
H7b	None found	Exons 2-4 skipped

^aLower case letters designate intron sequences. The intron in which the mutation occurs is noted, and the location of the mutated nucleotide is given relative to the nearest exon, with negative numbers being 5' of the exon and positive numbers being 3' of the exon.

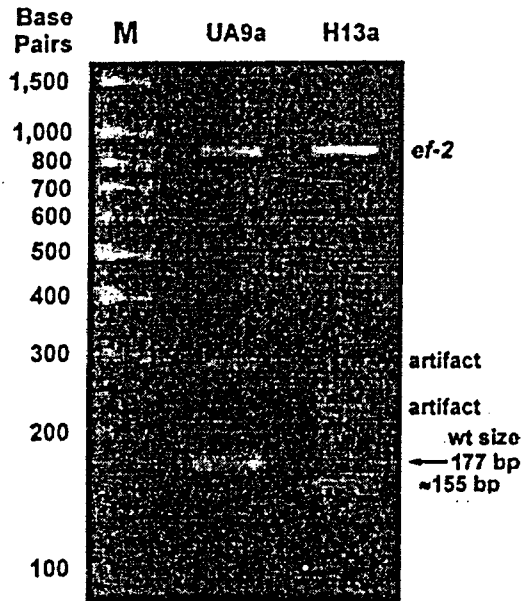


Figure 3. Multiplex PCR of CHO EM9 exon 4 genomic DNA with *ef-2* as the internal standard. The H13a exon 4 fragment size was estimated to be about 155 base-pairs in size when compared to both the 177-base wild-type amplicon (UA9a) and a 100-base-pair ladder (M). Mutant UA9a has exons 6–9 deleted from its genomic DNA but exon 4 is intact.

exon 1 (Table 5); the cumulative effect of these mutations may have resulted in the cDNA phenotype observed.

DISCUSSION

The various mutations identified (Tables 3–5) were combined into categories of presumed genomic

perturbations for spontaneous, UA-treated, and H₂O₂-treated CHO EM9 cells (Table 6). The resultant spectra were significantly different ($P < 0.001$). Of greatest relevance were differences between the UA-induced spectrum and each of the other spectra. The UA-induced mutation spectrum was significantly different from both the spontaneous ($P < 0.05$) and the H₂O₂-induced ($P < 0.01$) spectra, while the spontaneous and H₂O₂-induced spectra were also significantly different ($P < 0.001$).

A comparison of categories revealed significant differences between UA and both S and H for several types of mutations. UA produced significantly fewer 1–22 base deletions than generated either spontaneously ($P < 0.05$) or by H₂O₂ ($P < 0.05$). UA also induced significantly more 1–2 base insertions than generated spontaneously ($P < 0.05$) but significantly fewer than elicited by H₂O₂ ($P < 0.05$). Also, the frequency of UA-induced mutations possibly because of major genomic rearrangements (insertions and deletions of more than one exon) was significantly greater than in spontaneous mutations ($P < 0.05$). However, the percentage of UA-induced base substitutions possibly because of oxidative damage was not significantly different than in spontaneously generated or H₂O₂-induced mutants.

The levels of mutations possibly induced by reactive oxygen species (ROS) in UA-, H₂O₂-, and spontaneously-generated mutants were compared to each other and to published data to assess involvement of ROS in UA-induced mutagenesis. Huo et al. inferred that point mutations at the CHO *hprt* locus in bystander cells that are near cells exposed to low level alpha particle irradiation are caused by ROS [53]; however, those mutants are screened by amplifying genomic DNA and visualizing the amplicons on agarose gels, and what is labeled "point

Table 6. Comparison of UA-Induced, Spontaneous, and H₂O₂-induced *hprt* Mutations Generated in CHO EM9

Mutations	UA-induced (59 mutations)	Spontaneous (38 mutations)	H ₂ O ₂ -induced (45 mutations)
Base substitutions	18 (30.5%)	16 (42.1%)	7 (15.6%)
Transitions	6 (10.2%)	4 (10.5%)	1 (2.2%)
Transversions	12 (20.3%)	12 (31.6%)	6 (13.3%)
G → T or C → A	8 (13.6%)	10 (26.3%)	3 (6.7%) ^a
Deletions	26 (44.1%)	20 (52.6%)	23 (51.1%)
Small (1–22 bp)	3 (5.1%) ^b	7 (18.4%)	9 (20.0%)
One exon ^c	9 (15.3%)	10 (26.3%)	3 (6.7%) ^a
Multiexon	9 (15.3%)	2 (5.3%)	9 (20.0%)
Whole-gene	5 (8.5%)	1 (2.6%)	2 (4.4%)
Insertions	15 (25.4%)	2 (5.3%)	15 (33.3%)
Small (1–2 bp)	9 (15.3%) ^b	1 (2.6%)	15 (33.3%) ^d
One exon	3 (5.1%)	0	0
Multiexon	3 (5.1%)	1 (2.6%)	0

^aSignificantly different from spontaneous ($P < 0.05$).

^bSignificantly different from spontaneous and H₂O₂-induced ($P < 0.05$).

^cExons 7 and 8 are considered a unit because of their proximity and that they are amplified from the genomic DNA as a single fragment.

^dSignificantly different from spontaneous ($P < 0.001$).

mutations" will have included small deletions and insertions as well as point mutations. In the current work, comparing the frequencies of "point mutations" as defined by Huo and co-workers with those in our three treatments, resulted in statistically insignificant differences of 51%, 63%, and 67% for UA-induced, spontaneously generated, and H₂O₂-induced mutations, respectively (Table 6). This suggested that ROS-induced mutations as defined by Huo et al. [53] could have contributed to mutagenesis in all three exposure conditions. However, this inclusion of small deletions and insertions as well as base substitutions could include more than ROS-mediated damage. This inference was further strengthened by analysis of base substitutions that could indicate the presence of 8-oxo-2-deoxyguanosine (8-oxodG) in spontaneously-generated and in UA- and H₂O₂-exposed cells.

The DNA lesion 8-oxodG is generally considered to be the most relevant marker for ROS. The base substitutions attributed to oxidative damage via the formation of 8-oxodG are substitutions of G → T and C → A (a G → T mutation on the complementary strand) [54]. There are other possible mechanisms to generate such substitutions, but these base substitutions are generally considered to indicate the proportion of mutations that may be attributable to oxidative damage.

ROS, and specifically generation 8-oxodG, have been presumed to play a role in spontaneously generated mutations. Xu and co-workers found that about 20% of the *hprt* mutations they characterized in CHO K1 cells passaged for 2–3 wk are G → T and C → A transversions [48], as compared to 26% for our cells passaged for 6 wk prior to selection with 6-TG. This suggested that the accumulation of such mutations could be proportional to the length of time the cultures were grown prior to mutant selection, and was consistent with the interpretation that these mutations were at least partially caused by metabolically generated oxygen radicals.

Involvement of 8-oxodG in H₂O₂-induced mutagenesis is less clear in the current study as well as in previous literature. Current results showed that there were significantly fewer G → T and C → A base substitutions in H₂O₂-induced than in spontaneous mutations ($P < 0.05$). The H₂O₂-induced mutations might have been expected to exhibit the largest proportion of oxidative damage; however, the current results are consistent with other studies that call into question the importance of 8-oxodG in dioxygen or H₂O₂-induced mutagenesis relative to ROS-induced clastogenicity [55–58].

Also, in the present work, the frequency of UA-induced G → T and C → A mutations was less than that of spontaneous mutations but greater than H₂O₂-generated mutations, although not significantly different from either group. This trend,

combined with the possibility that 8-oxodG generation may not be the most significant pathway for formation of H₂O₂-induced mutations suggested that 8-oxodG damage may be present in UA-exposed CHO cells, but is not necessarily the major pathway for UA-induced mutagenesis under these conditions. This interpretation is also consistent with our previous study that found no significant levels of 8-oxodG in UA-exposed CHO cells with the comet assay with posttreatment exposure to formamido-pyrimidine glycosylase protein (FPG) [40].

The observation that UA produced significantly more major genomic rearrangements (multiexon insertions and deletions combined) than occurred spontaneously ($P < 0.05$) suggests that, aside from 8-oxodG, DNA strand breaks or crosslinks could also be UA-induced mutagenic lesions. Bleomycin, a radiomimetic that induces DNA double strand breaks, was found to produce large deletions in CHO K1-BH4 cells [59]. The mutational spectrum of the DNA-DNA interstrand crosslinker MMC at the *tk* locus of mouse-lymphoma L5178Y cells included mostly large multigenic deletions, consistent with its identification as a clastogen [60].

Experiments have begun to characterize UA-induced DNA lesions in CHO cells, and results are consistent with the currently reported mutation spectrum. DNA strand breaks and general uranium-DNA adducts have been observed in CHO EM9 and CHO AA8 cells; however, these adducts have not yet been differentiated in terms of uranium-containing DNA-protein crosslinks or uranium-containing DNA-DNA crosslinks [40]. DNA crosslinks across the phosphate backbone have been inferred to be present in oligonucleotides exposed to uranyl ion *in vitro* [61]; however, their presence has not yet been investigated in cells or animals. Further experiments are in progress to more fully characterize the DNA lesions induced by UA.

Data from the current study were also compared to literature data for mutations generated by alpha-particle and radon exposure to evaluate the possible contribution of radiation damage to UA-induced mutations. Schwartz et al. exposed CHO-K1 cells to alpha radiation with Bismuth-212, a radon daughter [42]. When our data were grouped into equivalent categories and compared to their data, the two profiles were different ($P < 0.00001$). The frequency of alpha-generated whole-gene deletions was significantly greater than that of UA-induced whole-gene deletions ($P < 0.000001$), but single exon and multi-exon deletions were not significantly different. However, this does not confirm the involvement of alpha irradiation because radiomimetic chemicals such as pesticides and bleomycin can induce chromosomal aberrations in the absence of radiation [62,63]. Therefore, although there may be an alpha-radiation component to the mutations observed in UA clones, this mutation pattern could also

be because of chemical rather than radiological mechanisms. Additionally, UA generated significantly more mutations in the "no exon deleted" category than alpha radiation ($P < 0.001$), suggesting alpha radiation may not be a major factor in UA-induced mutagenesis.

The observed UA-induced mutations were also distinct from those caused by radon exposure. Jostes et al. exposed CHO C18 cells to lower (0.25–0.3 Gy) and higher (0.75–0.77 Gy) levels of radon, and found that the mutation profile for lower radon exposures was not significantly different from the higher radon exposure [43]. They found that whole-gene deletions (defined as deletions of either exons 1–9 or 2–9) were significantly more frequent in radon-induced than in spontaneous mutations [43]. In the current study, no significant differences between whole-gene deletions in spontaneous and UA-induced mutants were found. It is possible that the lower induction rate of 2.8 in the current study compared to at least 9 in the radon study [43] resulted in our inability to detect a difference between our UA-induced and spontaneous mutations. However, the UA spectrum was significantly different from both the radon and spontaneous spectrum of Jostes and coworkers ($P < 0.00001$ and $P < 0.01$, respectively) [43], suggesting there may well be differences between radon- and UA-induced mutations in spite of our relatively high background.

In summary, differences between the UA-generated mutation spectrum and spectra generated spontaneously, by H_2O_2 , and by alpha and beta particles suggested that UA has distinct effects on cells that result in a mutagenic response. UA induced significantly more major genomic rearrangements than were generated spontaneously. Furthermore, significant differences between mutations generated by UA and generated spontaneously or by H_2O_2 exposure suggested that UA may have a reactivity with DNA that is not limited to free radical generation. These data were also not consistent with a simple radiological mechanism, because the UA spectrum was significantly different from reported alpha- and radon-generated spectra, and the EM9 line was not found to be more sensitive to hprt mutations induced by X-rays or alpha particles than the parental AA8 line [41] but UA was more mutagenic in EM9 cells than AA8 cells [40]. The summation of these data suggests that uranium, although radioactive, may also act as a heavy metal to generate DNA damage.

ACKNOWLEDGMENTS

Funding for this work was provided by the Native American Cancer Research Partnership through NIH grant CA096320 (D.M.S.). Equipment was purchased through the Arizona Board of Regents Biotechnology and Human Welfare Program (D.M.S.). NIH Grant CA096320 (D.M.S.).

REFERENCES

1. ATSDR (Agency for Toxic Substances and Disease Registry). Toxicological profile for uranium (update). Atlanta, GA: Public Health Service; 1999.
2. Churchill W. From a Native Son: Selected Essays in Indigenism, 1985-1995. Cambridge, MA: South End Press; 1996. p. 231.
3. Brugge D, Goble R. The history of uranium mining and the Navajo people. *Am J Public Health* 2002;92:1410–1419.
4. Mitchel RE, Sunder S. Depleted uranium dust from fired munitions: Physical, chemical and biological properties. *Health Phys* 2004;87:57–67.
5. Kalinich JF, Ramakrishnan N, Villa V, McClain DE. Depleted uranium-uranyl chloride induces apoptosis in mouse J774 macrophages. *Toxicology* 2002;179:105–114.
6. McDiarmid MA, Squibb K, Engelhardt SM. Biologic monitoring for urinary uranium in gulf war I veterans. *Health Phys* 2004;87:51–56.
7. Durakovic A. Undiagnosed illnesses and radioactive warfare. *Croatian Med J* 2003;44:520–532.
8. McDiarmid MA, Hooper FJ, Squibb K, McPhaul K. The utility of spot collection for urinary uranium determinations in depleted uranium exposed Gulf War veterans. *Health Phys* 1999;77:261–264.
9. McDiarmid MA, Keogh JP, Hooper FJ, McPhaul K, Squibb K, Kane R, et al. Health effects of depleted uranium on exposed Gulf War veterans. *Environ Res* 2000;82:168–180.
10. McDiarmid MA, Engelhardt SM, Oliver M. Urinary uranium concentrations in an enlarged Gulf War veteran cohort. *Health Phys* 2001;80:270–273.
11. McDiarmid MA, Squibb K, Engelhardt S, Oliver M, Gucer P, Wilson PD, et al. Depleted Uranium Follow-Up Program. Surveillance of depleted uranium exposed Gulf War veterans: Health effects observed in an enlarged "friendly fire" cohort. *J Occup Environ Med* 2001;43:991–1000.
12. Hodge SJ, Ejnik J, Squibb KS, McDiarmid MA, Morris ER, Landauer MR, et al. Detection of depleted uranium in biological samples from Gulf War veterans. *Mil Med* 2001;166:69–70.
13. McDiarmid MA, Hooper FJ, Squibb K, McPhaul K, Engelhardt SM, Kane R, et al. Health effects and biological monitoring results of Gulf War veterans exposed to depleted uranium. *Mil Med* 2002;167:123–124.
14. Gwiazda RH, Squibb K, McDiarmid M, Smith D. Detection of depleted uranium in urine of veterans from the 1991 Gulf War. *Health Phys* 2004;86:12–18.
15. McDiarmid MA, Engelhardt S, Oliver M, Gucer P, Wilson PD, Kane R, et al. Health effects of depleted uranium on exposed Gulf War veterans: A 10-year follow-up. *J Toxicol Environ Health A* 2004;67:277–296.
16. Horan P, Dietz L, Durakovic A. The quantitative analysis of depleted uranium isotopes in British, Canadian, and U.S. Gulf War veterans. *Mil Med* 2002;167:620–627.
17. Ough EA, Lewis BJ, Andrews WS, Bennett LG, Hancock RG, Scott K. An examination of uranium levels in Canadian forces personnel who served in the Gulf War and Kosovo. *Health Phys* 2002;82:527–532.
18. Macfarlane GJ, Biggs AM, Maconochie N, Hotopf M, Doyle P, Lunt M. Incidence of cancer among UK Gulf war veterans: Cohort study. *BMJ* 2003;327:1373.
19. Bem H, Bou-Rabee F. Environmental and health consequences of depleted uranium use in the 1991 Gulf War. *Environ Int* 2004;30:123–134.
20. Gottlieb LS, Husen LA. Lung cancer among Navajo uranium miners. *Chest* 1982;81:449–452.
21. Samet JM, Kutvirt DM, Waxweiler RJ, Key CR. Uranium mining and lung cancer in Navajo men. *N Engl J Med* 1984;310:1481–1484.
22. Roscoe RJ, Deddens JA, Salvan A, Schnorr TM. Mortality among Navajo uranium miners. *Am J Public Health* 1995;85:535–540.

23. Silver K. The yellowed archives of yellowcake. *Public Health Rep* 1996;111:116-127.
24. Gilliland FD, Hunt WC, Pardilla M, Key CR. Uranium mining and lung cancer among Navajo men in New Mexico and Arizona, 1969 to 1993. *J Occup Environ Med* 2000;42:278-283.
25. Mulloy KB, James DS, Mohs K, Kornfeld M. Lung cancer in a nonsmoking underground uranium miner. *Environ Health Perspect* 2001;109:305-309.
26. Mason TJ, Fraumeni JF, Jr., McKay FW, Jr. Uranium mill tailings and cancer mortality in Colorado. *J Natl Cancer Inst* 1972;49:661-664.
27. Wilkinson GS. Gastric cancer in New Mexico counties with significant deposits of uranium. *Arch Environ Health* 1985;40:307-312.
28. Shields LM, Wiese WH, Skipper BJ, Charley P, Benally L. Navajo birth outcomes in the Shiprock uranium mining area. *Health Phys* 1992;63:542-551.
29. Au WW, Lane RG, Legator MS, Whorton EB, Wilkinson GS, Gabehart GJ. Biomarker monitoring of a population residing near uranium mining activities. *Environ Health Perspect* 1995;103:466-470.
30. Birchard K. Does Iraq's depleted uranium pose a health risk? *Lancet* 1998;351:657.
31. Aitken M. Gulf war leaves legacy of cancer. *BMJ* 1999;319:401.
32. Abu-Qare AW, Abou-Donia MB. Depleted uranium—The growing concern. *J Appl Toxicol* 2002;22:149-152.
33. Kapp C. WHO sends team to Iraq to investigate effects of depleted uranium. *Lancet* 2001;358:737.
34. Priest ND. Toxicity of depleted uranium. *Lancet* 2001;357:244-246.
35. Mould RF. Depleted uranium and radiation-induced lung cancer and leukaemia. *Br J Radiol* 2001;74:677-683.
36. Royal Society Working Group on the Health Hazards of Depleted Uranium Munitions. The health effects of depleted uranium munitions: A summary. *J Radiol Prot* 2002;22:131-139.
37. Sztajnkrycer MD, Otten EJ. Chemical and radiological toxicity of depleted uranium. *Mil Med* 2004;169:212-216.
38. Jostes RF. Genetic, cytogenetic, and carcinogenic effects of radon: A review. *Mutat Res* 1996;340:125-139.
39. Yazzie M, Gamble SL, Civitello ER, Stearns DM. Uranyl acetate causes DNA single strand breaks in vitro in the presence of ascorbate (vitamin C). *Chem Res Toxicol* 2003;16:524-530.
40. Stearns DM, Yazzie M, Bradley AS, Coryell VH, Shelley JT, Ashby A, Asplund CS, Lantz RC. Uranyl acetate induces *hprt* mutations and uranium-DNA adducts in Chinese hamster ovary EM9 cells. *Mutagenesis* 2005, in press.
41. Schwartz JL, Shadley JD, Atcher RW, Tang J, Whitlock JL, Rotmensch J. Comparison of radon-daughter-induced effects in repair-proficient and repair-deficient CHO cell lines. *Environ Mol Mutagen* 1990;16:178-184.
42. Schwartz JL, Rotmensch J, Sun J, An J, Xu Z, Yu Y, et al. Multiplex polymerase chain reaction-based deletion analysis of spontaneous, gamma ray- and alpha-induced *hprt* mutants of CHO-K1 cells. *Mutagenesis* 1994;9:537-540.
43. Jostes RF, Fleck EW, Morgan TL, Stiegler GL, Cross FT. Southern blot and polymerase chain reaction exon analyses of *HPRT*-mutations induced by radon and radon progeny. *Radiat Res* 1994;137:371-379.
44. Konecki DS, Brennan J, Fuscoe JC, Caskey CT, Chinault AC. Hypoxanthine-guanine phosphoribosyltransferase genes of mouse and Chinese hamster: Construction and sequence analysis of cDNA recombinants. *Nucleic Acids Res* 1982;10:6763-6775.
45. Rossiter BJ, Fuscoe JC, Muzny DM, Fox M, Caskey CT. The Chinese hamster *HPRT* gene: Restriction map, sequence analysis, and multiplex PCR deletion screen. *Genomics* 1991;9:247-256.
46. Yang JL, Maher VM, McCormick JJ. Amplification and direct nucleotide sequencing of cDNA from the lysate of low numbers of diploid human cells. *Gene* 1989;83:347-354.
47. Nakanishi T, Kohno K, Ishiura M, Ohashi H, Uchida T. Complete nucleotide sequence and characterization of the 5'-Flanking Region of mammalian elongation factor 2 Gene. *J Biol Chem* 1988;263:6384-6391.
48. Xu Z, Yu Y, Gibbs RA, Caskey CT, Hsie AW. Multiplex DNA amplification and solid-phase direct sequencing for mutation analysis at the *hprt* locus in Chinese hamster cells. *Mutat Res* 1993;288:237-248.
49. Snedecor GW, Cochran WG. *Statistical methods*, seventh edition. Ames, IA: Iowa State University Press; 1980. p 208-210.
50. Zar JH. *Biostatistical analysis*, second edition. Englewood Cliffs, NJ: Prentice-Hall, Inc.; 1984. p 52-53.
51. Wei SJ, Chang RL, Bhachech N, Cui XX, Merkle KA, Wong CQ, et al. Dose-dependent differences in the profile of mutations induced by (+)-7R,8S-dihydroxy-9S,10R-epoxy-7,8,9,10-tetrahydrobenzo(a)pyrene in the coding region of the hypoxanthine (guanine) phosphoribosyltransferase gene in Chinese hamster V-79 cells. *Cancer Res* 1993;53:3294-3301.
52. O'Neill JP, Rogan PK, Cariello N, Nicklas JA. Mutations that alter RNA splicing of the human *HPRT* gene: A review of the spectrum. *Mutat Res* 1998;411:179-214.
53. Huo L, Nagasawa H, Little JB. *HPRT* mutants induced in bystander cells by very low fluences of alpha particles result primarily from point mutations. *Radiat Res* 2001;156:521-525.
54. Cheng KC, Cahill DS, Kasai H, Nishimura S, Loeb LA. 8-Hydroxyguanine, an abundant form of oxidative damage, causes GT and AC substitutions. *J Biol Chem* 1992;267:166-172.
55. Rothfuss A, Stahl W, Radermacher P, Speit G. Evaluation of mutagenic effects of hyperbaric oxygen (HBO) in vitro. *Env Mol Mutagen* 1999;34:291-296.
56. Rothfuss A, Merk O, Radermacher P, Speit G. Evaluation of mutagenic effects of hyperbaric oxygen (HBO) in vitro. II. Induction of oxidative damage and mutations in the mouse lymphoma assay. *Mutat Res* 2000;471:87-94.
57. Bradley MO, Erickson LC. Comparison of the effects of hydrogen peroxide and X-ray irradiation on toxicity, mutation, and DNA damage/repair in mammalian cells (V79). *Biochim Biophys Acta* 1981;654:135-141.
58. Speit G. The relationship between the induction of SCEs and mutation in Chinese hamster cells. I. Experiments with hydrogen peroxide and caffeine. *Mutat Res* 1986;174:21-26.
59. An J, Trieff NM, Hsie AW. PCR-directed DNA sequencing of "nondeletion" *HPRT*-mutants induced by bleomycin in CHO K1-BH4 cells. *Environ Mol Mutagen* 1998;32:244-250.
60. Davies MJ, Phillips BJ, Rumsby PC. Molecular analysis of mutations at the *tk* locus of L5178Y mouse-lymphoma cells induced by ethyl methanesulphonate and mitomycin C. *Mutat Res* 1993;290:145-153.
61. Nielsen PE, Hiort C, Sönnichsen SH, Buchardt O, Dahl O, Nordén B. DNA binding and photocleavage by uranyl(VI) (UO_2^{2+}) salts. *J Am Chem Soc* 1992;114:4967-4975.
62. Bolzan AD, Bianchi NO, Laramendy ML, Bianchi MS. Chromosomal sensitivity of human lymphocytes to bleomycin. Influence of antioxidant enzyme activities in whole blood and different blood fractions. *Cancer Genet Cytogenet* 1992;64:133-138.
63. Garaj-Vrhovac V, Zeljezic D. Assessment of genome damage in a population of Croatian workers employed in pesticide production by chromosomal aberration analysis, micronucleus assay and Comet assay. *J Appl Toxicol* 2002;22:249-255.

UNITED STATES OF AMERICA
NUCLEAR REGULATORY COMMISSION

In the Matter of)	Docket No. 40-8838-MLA
)	
U.S.ARMY)	ASLBP No. 00-776-04-MLA
)	
(Jefferson Proving Ground Site))	June 30, 2006

CERTIFICATE OF SERVICE

I hereby certify that copies of the foregoing "Motion for Leave to Further Supplement Contentions of Save the Valley, Inc. Within Sixty (60) Days" has been served this 30st day of June, 2006, upon the following persons by electronic mail and by U.S. Mail, first class postage prepaid.

Administrative Judge Alan S. Rosenthal, Chair
Atomic Safety and Licensing Board Panel
U.S. Nuclear Regulatory Commission
Mail Stop: T-3-F-23
Washington, D.C. 20555-0001

Adjudicatory File
Atomic Safety and Licensing Board
U.S. Nuclear Regulatory Commission
Mail Stop: T-3-F-23
Washington, D.C. 20555

Administrative Judge Paul B. Abramson
Atomic Safety and Licensing Board Panel
U.S. Nuclear Regulatory Commission
Mail Stop: T-3-F-23
Washington, D.C. 20555

Larry D. Manecke, Commander
Rock Island Arsenal
ATTN: AMSTA-RI-GC (L.MANECKE)
One Rock Island Arsenal
Rock Island, IL 61299-5000

Administrative Judge Richard F. Cole
Atomic Safety and Licensing Board Panel
U.S. Nuclear Regulatory Commission
Mail Stop: T-3-F-23
Washington, D.C. 20555

John J. Welling, Chief Counsel
Rock Island Arsenal
ATTN: AMSTA-RI-GC (J.WELLING)
One Rock Island Arsenal
Rock Island, IL 61299-5000

Frederick P. Kopp
U.S. Army Garrison - Rock Island Arsenal
Office of Counsel (AMSTA-RI-GC)
One Rock Island Arsenal
Rock Island, IL 61299-5000

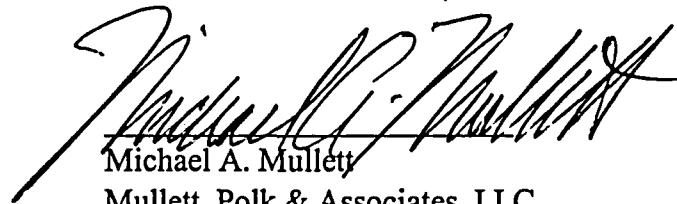
Office of the Secretary
ATTN: Rulemaking and Adjudications Staff
U.S. Nuclear Regulatory Commission
Mail Stop: O-16-G-15
Washington, D.C. 20555-0001

Patrick A. Moulding
Marian L. Zobler
Sara E. Brock
Margaret J. Bupp
Harry E. Wedewer
Office of the General Counsel
U.S. Nuclear Regulatory Commission 0-15D21
Washington, DC 20555-0001

Office of Commission Appellate Adjudication
U.S. Nuclear Regulatory Commission
Mail Stop: O-16-G-15
Washington, D.C. 20555-0001

Tom McLaughlin, Decommissioning Branch
Division of Waste Management
Office of Nuclear Materials and Safeguards
U.S. Nuclear Regulatory Commission
Washington, DC 20555-0001

Richard Hill, President
Save The Valley
P.O. Box 813
Madison, IN 47250



Michael A. Mullett
Mullett, Polk & Associates, LLC
309 West Washington Street, Suite 233
Indianapolis, IN 46204
Phone: (317) 636-5165
Fax: (317) 636-5435
E-mail: mmullett@mullettlaw.com

Attorney for Save the Valley, Inc.

MULLETT, POLK & ASSOCIATES, LLC

ATTORNEYS AT LAW
Old Trails Building, Suite 233
309 West Washington Street
Indianapolis, Indiana 46204-2721
Tel:(317) 636-5165 / Fax: 317-636-5435

*Michael A. Mullett, Senior Counsel
Jerome E. Polk, Lead Counsel*

June 30, 2006

Secretary
U.S. Nuclear Regulatory Commission
Washington, D.C. 20555-0001
ATTN: Rulemakings and Adjudications Staff

Re: Reply in Support of Motion for Leave to Withdraw, Amend and Supplement Contentions and Final Contentions of Save the Valley, Inc.

Motion for Leave to Further Supplement Contentions within Sixty (60) Days of Save the Valley, Inc.

In the Matter of the U.S. Army (Jefferson Proving Ground Site), Docket No. 40-8838-MLA, ASLBP 00-776-04-MLA

Dear Secretary:

Enclosed please find for filing in the above-referenced docket the original and two conformed copies of the (1) Reply in Support of Motion for Leave to Withdraw, Amend and Supplement Contentions and Final Contentions of Save the Valley, Inc. and the related Certificate of Service, and (2) Motion for Leave to Further Supplement Contentions within Sixty (60) Days of Save the Valley, Inc., with attachments and the related Certificate of Service.

Thank you for your assistance in this matter.

Respectfully submitted,



Michael A. Mullett
Attorney for Save the Valley, Inc.

cc: Service List – Docket No. 40-8838, ASLBP 00-776-04